DIFFRACTION PATTERN ANALYSIS OF BRIGHT TRACE FLARES

ANDREW C. LIN[1], RICHARD W. NIGHTINGALE[2,*] and THEODORE D. TARBELL[2]
[1]*Palo Alto High School, 50 Embarcadero Road, Palo Alto, CA 94301, U.S.A.*
(e-mail: aclin@fas.harvard.edu)
[2]*Lockheed Martin Advanced Technology Center, Solar & Astrophysics Laboratory, Orgn. L9-41, Bldg. 252, 3251 Hanover St., Palo Alto, CA 94304, U.S.A.*
(e-mails: nightingale@lmsal.com; tarbell@lmsal.com)

(Received 13 September 2000; accepted 16 October 2000)

Abstract. A study of the diffraction patterns seen in TRACE images of bright flare kernels was undertaken to better understand the properties of the telescope. The diffraction pattern caused by light from a bright flare kernel passing through the mesh supporting the filters at the front of the TRACE telescope has been examined, and a method has been developed to use this pattern to determine the zeroth order intensity of flares that cannot be measured directly due to saturation of the Analog to Digital Converter (ADC) in the CCD detection package. The validity of this method is confirmed by testing it on a flare that does not saturate the ADC. The diffraction pattern allows us to measure intensities far brighter than the detection package allows; the range has been effectively increased by at least 41 times. The light scattered from any point was observed to be $\approx$ 20%, a significant amount which may be affecting the image quality of the telescope. An accurate determination of the ratio of the square slit size to slit spacing of the wire mesh was obtained. Wavelength dispersion, the phenomenon that as the higher-order diffracted peaks lie further from the center, they spread out until double peaks are observed, has also been examined. This effect is caused by two principal wavelengths, Fe IX at 171.073 Å and Fe X at 174.507 Å in the TRACE 171 Å passband. This study is a part of the TRACE Team educational outreach program.

1. Extrapolating the Flare Intensity from the Diffraction Pattern

1.1. INTRODUCTION

The Transition Region and Coronal Explorer satellite, TRACE, launched 2 April 1998, images the solar photosphere, transition region and corona with high spatial (1 arc sec) and temporal resolution at EUV, UV and white light continuum wavelengths (Handy *et al.*, 1999; Schrijver *et al.*, 1999). Thin-film aluminum filters, supported by nickel mesh, exclude visible light in the 3 EUV quadrants at the entrance to the telescope. The mesh diffracts the incoming EUV light and produces obvious diffraction patterns when the light becomes intense enough, such as from a bright flare kernel.

We use the brightness and spacing of the diffraction pattern to determine the intensity of the flare kernel that creates it. This is often necessary because the flare

*Author for correspondence

Solar Physics **198:** 385–398, 2001.

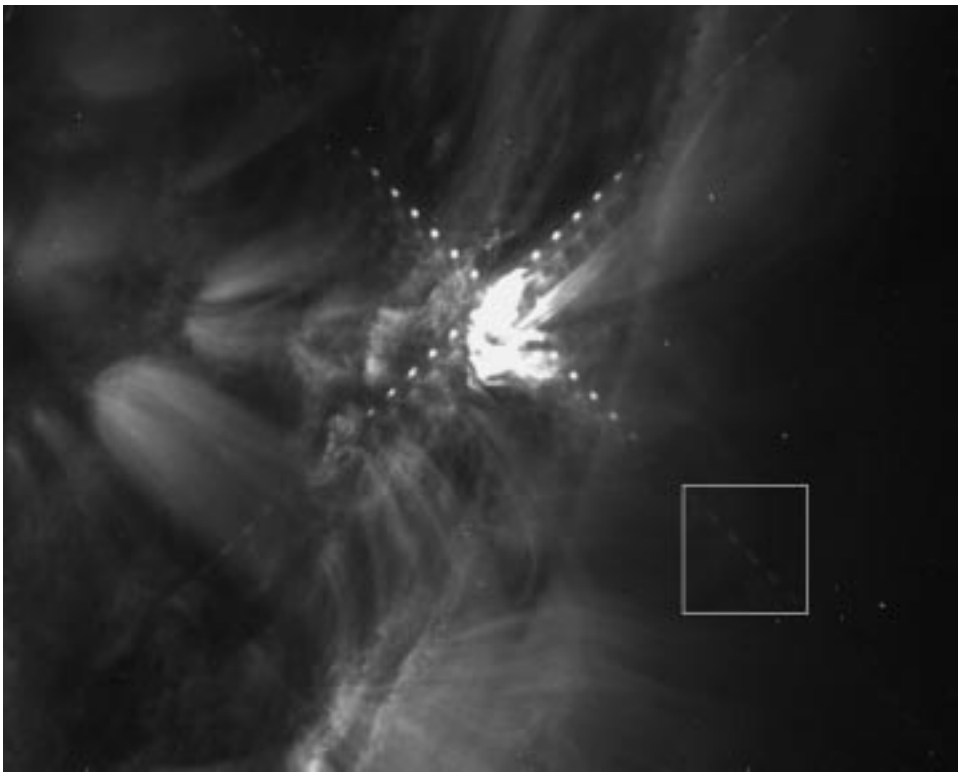

Figure 1. The 16 May 1999 diffraction pattern is shown. The dots fade out at the 9th order, then brighten again, then fade again to the 18th order, and brighten and fade again. There are 23 visible orders. (The very faint dots are barely visible in the lower left and lower right corners.) The area enclosed by the white box is magnified in Figure 7.

is so bright that it saturates the 12-bit capacity of the Analog to Digital Converter (ADC) of the CCD camera. This method allows us to greatly increase the dynamic range of the instrument.

We observed such a flare on 16 May 1999 at 13:49:21 UT. The diffraction pattern is shown in Figure 1. Another example of a flare can be seen on 15 March 2000 at 18:38:40 UT. The diffraction pattern of this flare can be seen in Figure 2. The flare is bright enough to produce a diffraction pattern but not enough for the zeroth order to saturate the ADC. This can be used to validate the results from the first flare. The diffraction pattern is due to the Ni mesh, depicted in Figure 3, that supports the aluminum filter at the front of the telescope. The mesh acts like a two dimensional grating and diffracts the incoming light.

1.2. MATHEMATICAL TREATMENT

We can represent the mesh by a two-dimensional series of square slits. In each dimension, this can be represented as a series of slits, such as shown in Figure 4.

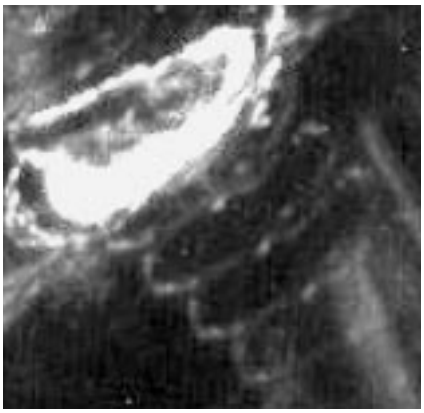

Figure 2. The 15 March 2000 diffraction pattern is displayed.

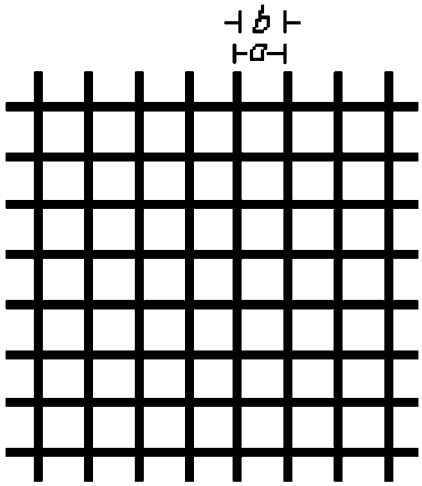

Figure 3. A schematic of the Ni mesh is shown; a is the distance between openings and b is the width of each opening.

We consider the following parameters:

θ = the angle that the light is diffracted by – the angle between the light ray and the line perpendicular to the mesh;
a = the distance between slits;
b = the width of each slit;
N = the total number of slits;
λ = the wavelength of the light (171 Å);
$k = \frac{2\pi}{\lambda}$;
m = the order number;
We define $\alpha = \frac{ka}{2} \sin\theta$ and $\beta = \frac{kb}{2} \sin\theta$.

The relevant specifications of the TRACE telescope front filter mesh are as follows: there are 70 lines per inch, i.e., $a = 3.63 \times 10^{-4}$ m; the transmission

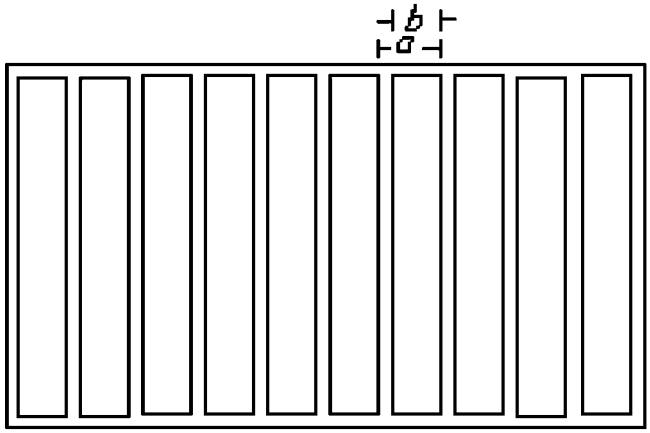

Figure 4. A diagram of a representation of the mesh in one dimension as a series of slits is shown.

of the mesh is 82%; and each pixel has a spatial span, or resolution, of 0.50 arc seconds (Handy *et al.*, 1999).

The following equation describes the light intensity distribution after passing through a series of slits, such as on a grating (Hecht and Zajac, 1974):

$$I(\theta) = I_0 \left(\frac{\sin\beta}{\beta}\right)^2 \left(\frac{\sin N\alpha}{\sin\alpha}\right)^2. \tag{1}$$

At each principal maximum $\alpha = m\pi$, where m is the order number, so

$$\left(\frac{\sin N\alpha}{\sin\alpha}\right)^2 = N^2 \tag{2}$$

and $((\sin\beta)/\beta)^2$ is the term which determines the intensity we see in the principal maxima. To find out what $((\sin\beta)/\beta)^2$ is at each peak, we must solve for β in terms of m, the order number. Since $\beta = (b/a)\alpha$, $\beta_m = m\pi b/a$. Substituting for β in Equation (1), and using Equation (2), we get

$$I(m) = I_0 \left(\frac{\sin(m\pi b/a)}{m\pi b/a}\right)^2 N^2, \tag{3}$$

or, with $I_0 = I(0)/N^2$ at zeroth order,

$$I(0) = \frac{I(m)}{\left(\dfrac{\sin(m\pi b/a)}{m\pi b/a}\right)^2}. \tag{4}$$

This equation relates the zeroth order intensity with that of any of the other orders.

According to this theoretical description, the only parameter needed to apply Equation (4) is the value of b/a. A simple numerical calculation adding up orders

from 1 to 23 shows that if light is diffracted in four directions as observed in the 16 May flare, 20.0% of the light is diffracted away from the zeroth order.

1.3. METHOD

We want to find the intensities of each peak in the diffraction pattern, to see if the data match the theoretical expectation of Equation (4), and if they do, to extrapolate the zeroth order flare intensity. But because the dots become wider and even split into double images (see Section 2), we cannot just measure the highest pixel in each peak. Therefore, we summed up the intensities of all the pixels in each bright spot, subtracting from each pixel the mean background intensity near each bright spot to ignore other light coming from the sun unrelated to the diffraction pattern.

The 15 March flare is dimmer and its shape is more nebulous. To reduce errors coming from measuring intensities over different sized areas for different peaks, we fixed the number of pixels for each order at 33. Dispersion has only a small effect because we examined only the first three orders. Otherwise, we measured the intensities by the same method. The zeroth order also has to have the background taken into account, because any intense background around the zeroth order of the flare will also be diffracted to become background around the higher orders.

To find the value of b/a, we analyzed the data to see where the intensity of the peaks drops to zero. Since the term $\left(\frac{\sin(m\pi b/a)}{m\pi b/a}\right)^2$ is what modulates the peaks, that term would go to 0 when the sine goes to zero, that is, when mb/a is a whole number. In actual practice this may occur near, but in between, m-values. We can use the diffraction pattern data to determine the best fit of the zeroes.

The highest pixel of each order, $I_{\max}$, will have a certain ratio to the full intensity of the order, I_{tot}, and it will decrease as the order increases and the dots become wider. To estimate how $I_{\max}(0)$ relates to $I_{\text{tot}}(0)$, we found $I_{\max}$ for each order and compared it to I_{tot}.

1.4. RESULTS FOR THE 16 MAY FLARE

Table I shows the data where $+45$, etc., indicate the direction of the arm of the diffraction pattern; $+45$ indicates 45 degrees up from right, -45 indicates 45 degrees down from right, etc. The spacing of the orders along each arm is about 20 pixels or 10 arc sec.

The value of b/a: Analyzing the data, we see that the intensity of the peaks drops to zero slightly before the 9th order (because the 8th order is much dimmer than the 10th order), and right between the 17th and 18th orders. So the intensity vanishes close to every 9 orders. We conclude that b/a must be close to an even fraction of 9, such as $\frac{7}{9}$, $\frac{5}{9}$, etc. The transmission of the mesh is 82%, and since b is the width of the opening and a is the distance between openings, $(b/a)^2 = 0.82$, or $b/a \approx 0.905$. The value that best fits the zeroes of the orders is 0.885.

TABLE I
Intensities of each peak in the diffraction pattern: 16 May 1999

order# (m)	$+45$	$+135$	-135	-45	Average	St. dev.
1	20578.4	20235	27072	25751.2	23409	3511
2	20779.8	18306	20992	–	20026	1493
3	18612.2	17100	13721.6	13161.4	15649	2632
4	11919.6	11960	13790	11586.4	12314	998
5	6980.4	7954	6177.6	6901.2	7003	729
6	3697.4	3650	2705	3908.8	3490	535
7	1016.4	1352	1584	1028.5	1245	274
8	–	171.5	–	91.2	131	57
9	0	0	0	0	0	–
10	345.6	399	262.5	324	333	57
11	699.6	907.2	815	489.6	728	180
12	985.8	1440	1170	980	1144	216
13	984	1505	1320	817.6	1157	312
14	608	837	745.2	562.5	688	125
15	–	–	800	365.7	583	307
16	–	–	0	0	0	–
17	–	–	0	0	0	–
18	–	–	0	0	0	–
19	–	–	0	0	0	–
20	–	–	253	255	254	1.4
21	–	–	279	245.7	262	34
22	–	–	204	202.1	203	2.3
23	–	–	369.6	–	369.6	–

Figure 5 shows that the theoretical curve fits the data very well. This leads us to believe that the theoretical representation of the diffraction pattern is correct.

Using Equation (4), we can take any order peak intensity as $I(m)$, and divide by the modulating function to find $I(0)$. We used the first seven orders to calculate an average extrapolated value for $I(0)$ (see Table II). We obtain an average result of $I(0) = 1.45 \times 10^6$. The uncertainty of the mean is 6.10×10^4, about 4.2% of the calculated value.

We must keep in mind that the zeroth order does not give the actual intensity of the flare, only the largest portion of it. Much of the light is diffracted off into the diffraction pattern, so to find the actual intensity of the flare, we have to add together all the orders. This gives us $1.45 \times 10^6 + 3.56 \times 10^5$, which is 1.81×10^6.

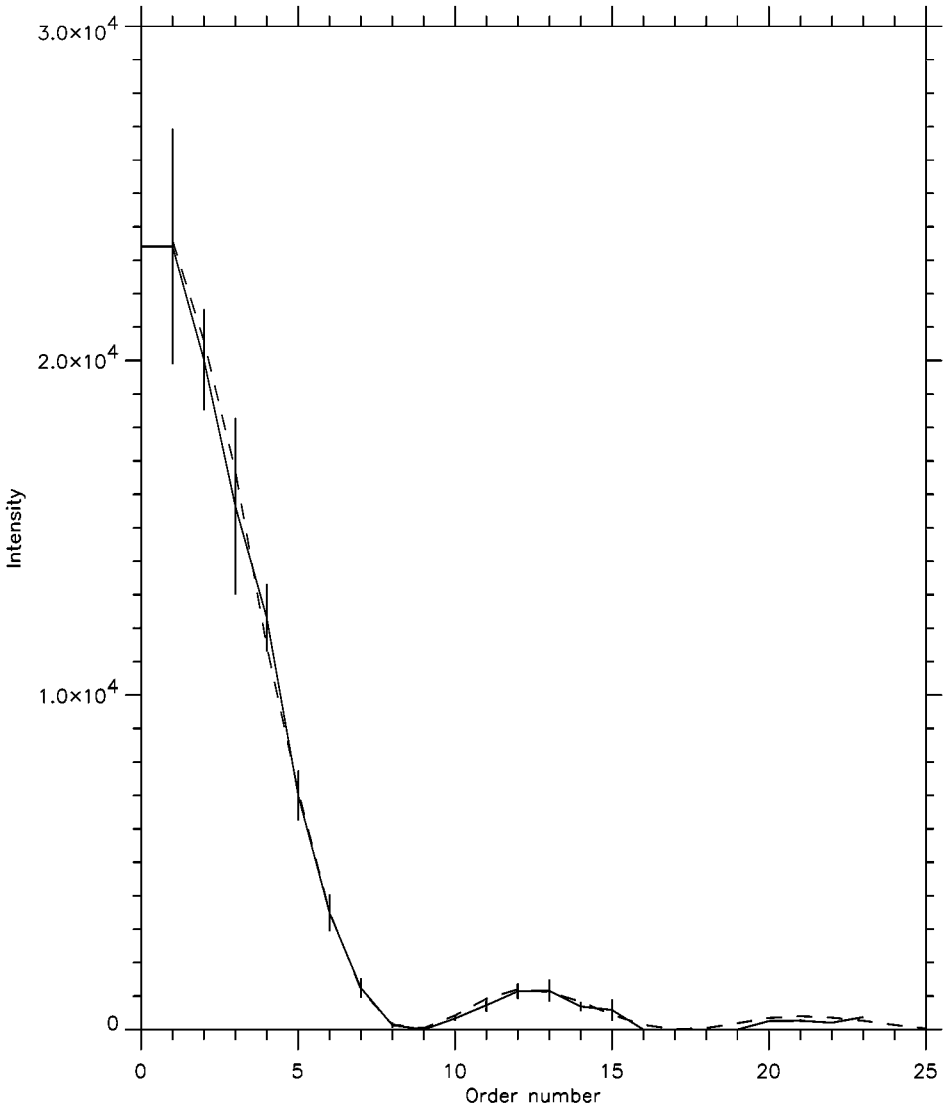

Figure 5. A comparison of the theoretical and observed intensities versus order number is shown. The *dashed line* represents the theoretical intensities $I(m) = I(0)\left(\frac{\sin(m\pi b/a)}{m\pi b/a}\right)^2$ (where $b/a = 0.885$). The *solid line* connects the measured intensities. The vertical bars represent the standard deviations at each of the observed orders.

TABLE II

Predicted intensity of zeroth order for the 16 May, 1999 flare

Order No.	Average $I(m)$	Predicted $I(0)$ (by Equation (4))
1	23409	1.45×10^6
2	20026	1.42×10^6
3	15649	1.39×10^6
4	12314	1.55×10^6
5	7003	1.43×10^6
6	3490	1.42×10^6
7	1245	1.43×10^6

TABLE III

Comparing $I_{\max}$ and I_{tot}, at each order in the 16 May, 1999 diffraction pattern

Order No.	Average $I_{\max}$	Average I_{tot}	$I_{\text{tot}}/I_{\max}$
1	2610	23409	8.97
2	2127	20026	9.42
3	1515	15649	10.30
4	970	12314	12.70
5	524	7003	13.37
6	228	3490	15.30
7	69	1245	18.11

Significantly, the total intensity of the entire 16 May diffraction pattern through 23 orders is $19.7 \pm 0.3\%$ of the intensity of the flare. The error is derived from the standard deviations of each order. This means that $\approx$ 20% of all the light coming through the filter is diffracted away from its original angle, even when the diffraction pattern is too dim to be visible. Also, this indicates that $\approx$ 20% of the light is being lost from the zeroth order position and being spread out over the entire image.

Now we examine how the intensity range of the camera has been increased. Table III compares the intensity of the highest pixel, $I_{\max}$, to the total intensity, I_{tot}, at each order for the 16 May event.

The graph in Figure 6 shows that we can estimate that I_{tot} for the zeroth order is 8.7 times greater than $I_{\max}$. We conclude that the highest pixel value is $\frac{1.45 \times 10^6}{8.7}$, or 1.67×10^5. This means that our intensity range has been effectively increased

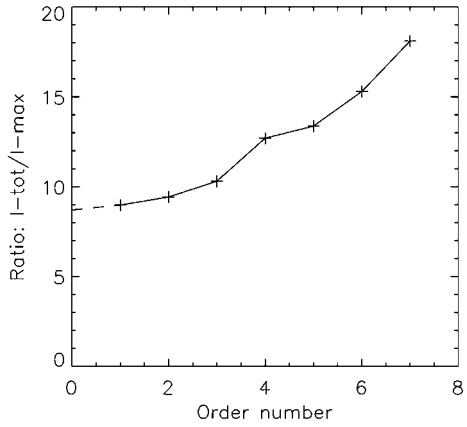

Figure 6. The ratio $I_{\mathrm{tot}}/I_{\mathrm{max}}$ as a function of order number m is shown; we extrapolate backwards to find the ratio for the 0th order.

by a factor of 41, from 1 : 4096 to $1 : 1.67 \times 10^5$. Furthermore, we can expect that we can still use this method to determine intensities of even brighter flares; even if the diffraction pattern itself saturates, we can use higher orders to determine all of the orders, and the total intensity of the flare.

1.5. Results from 15 March flare

Intensities of each order of the diffraction pattern are shown in Table IV. The average of the estimations of the zeroth order from the higher orders is 32693 ± 2796 ($\pm 8.6\%$), while the measured unsaturated zeroth order intensity is 33378, well within the range of predicted values.

2. Dispersion Effect

2.1. Introduction

We also investigated the phenomenon that as the order increases in the diffraction pattern, the dots smear out until after the 10th or so order, we are seeing double dots, as shown in Figure 7. This happens because the telescope mirror coatings reflect a small range of wavelengths around 173 Å, from about 170 to 175 Å, and there are two major wavelengths coming through, Fe IX at 171.073 Å and Fe X at 174.507 Å (Verner, Verner, and Ferland, 1996). Over many orders, the images separate through dispersion, because the longer wavelength is diffracted more than the shorter one.

2.2. Mathematical treatment

From Section 1, we know that at each peak $\alpha = m\pi$, and

TABLE IV

Intensities of each peak of the diffraction pattern: 15 March 2000

In the -45 direction:		
Order No.	Intensity	Predicted $I(0)$ (Equation 4)
1	582.8	36056.9
2	409.2	28931.4
3	365.8	32583.5
In the $+135$ direction:		
Order No.	Intensity	Predicted $I(0)$ (Equation 4)
1	505.3	31262.1
2	489.8	34630.0

Figure 7. The dispersion effect: higher orders separate into double dots because the filter passes two major wavelengths, Fe IX at 171.073 Å and Fe X at 174.507 Å, and the longer wavelength is diffracted more than the shorter one. This picture is magnified and brightened from the box in Figure 1.

$$\alpha = \frac{ka}{2}\sin\theta = \left(\frac{2\pi}{\lambda}\right)\frac{a}{2}\sin\theta = \frac{\pi a}{\lambda}\sin\theta = m\pi$$

or

$$\sin\theta = \frac{m\lambda}{a}.$$

But for very small angles, $\sin\theta \approx \theta$, and here, λ/a is of the magnitude of 1×10^{-4}, so

$$\theta \approx \frac{m\lambda}{a}. \tag{5}$$

This means that if we want to compare the angle of diffraction for 2 slightly different wavelengths,

$$\Delta\theta \approx m\frac{\Delta\lambda}{a}. \tag{6}$$

The separation between the peaks of the two wavelengths will therefore increase linearly with order number, with a slope of $\Delta\lambda/a$.

Using Equation (6) and the value for $a(= 3.63 \times 10^{-4}$ m) as found above in Section 1.3, we can calculate that the slope of the line should be

$$\frac{\Delta\lambda}{a} = \frac{1.74507 \times 10^{-8} - 1.71073 \times 10^{-8}}{3.63 \times 10^{-4}} = 9.460 \times 10^{-7}.$$

That is, the separation between the peaks of the two wavelengths will increase by 9.460×10^{-7} radians (0.195 arc sec) per order. The separation between the peaks should therefore increase by 0.390 pixels per order number.

2.3. METHOD

Data were taken by counting the pixels in the x and y directions separating the maximum pixels in each order. Although there is no discernible separation before the 10th order (i.e., there are not two distinct peaks), the dispersion will make the length longer than the width, and so the separation between the images is given by the length minus the width.

2.4. RESULTS AND ANALYSIS

Data are shown in Table V and plotted in Figure 8. In analyzing the graph in Figure 8, we must remember that orders before No. 10 are measured differently from those after No. 10. In the method used for higher orders, where there were distinctly separate peaks, there is a possible error of about a pixel either way in the X and Y directions. Thus, along the diagonal, there is a potential error of about a $\sqrt{2}$ (= 1.41) pixels. For the smaller orders, the errors are about twice as large.

As seen in Figure 8, a linear trend matches the data, and this line has exactly the slope calculated. Although most data points are higher than the line in orders 1–7, and many are below in orders 11–16, the line is well within the error bars; any differences can be accounted for by measurement error.

We were also interested in comparing the relative intensities of the Fe IX 171.073 Å and the Fe X 174.507 Å wavelengths for each order. However, this was not feasible for these data because at higher orders, where the images separate, the diffracted image becomes very small and dim, and background variation as a source of error becomes much larger compared to the intensity of the image. Efforts to compare the intensities resulted in no consistent relationship between the two wavelengths.

TABLE V

Separation of peaks vs. order number in the 16 May, 1999 diffraction pattern

Order No.	+45	+135	−135	−45	Average separation
1	0	0	0	0	0
2	1.36	0	0.75	0	1.05
3	3.20	1.41	2.15	0	2.25
4	3.58	2.15	4.22	1.41	2.84
5	2.82	2.82	4.39	0.67	2.68
6	4.27	3.56	3.46	2.20	3.37
7	4.90	4.27	4.97	2.44	4.15
8	–	–	–	–	–
9	–	–	–	–	–
10	–	–	–	–	–
11	3.61	3.91	–	5.10	4.2
12	4.24	4.24	3.61	3.54	3.9
13	5.00	4.24	5.00	5.66	5.0
14	4.24	5.67	6.40	5.66	5.5
15	5.66	5.32	5.85	5.66	5.6
16	–	–	6.40	6.40	6.4
17	–	–	–	–	–
18	–	–	–	–	–
19	–	–	–	–	–
20	–	–	–	–	–
21	–	–	8.49	7.81	8.15
22	–	–	9.22	8.90	9.1
23	–	–	9.22	9.22	9.2
24	–	–	10.63	–	10.6

A TRACE diffraction pattern has been modeled and an algorithm (T. Metcalf, private communication) has been developed that deconvolves the pattern from the TRACE images, ultilizing the ratio of the slit width to slit spacing of the front filter mesh, as found above. Not only does the algorithm help clean up an image, but more importantly it computes the EUV intensity in regions where the CCD is saturated. Although still in the experimental stage, the procedure is available as part of the TRACE IDL SolarSoft package (see routine TRACE_UNDIFFRACT.PRO).

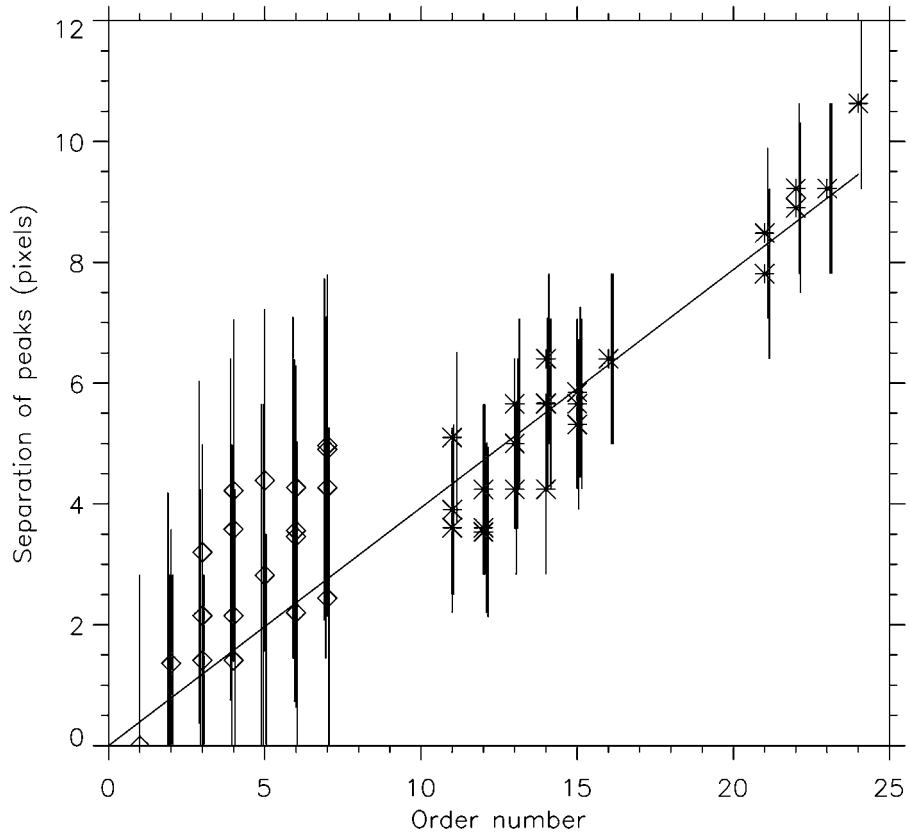

Figure 8. The separation between peaks is plotted against order number, with the vertical lines representing error bars (the error bars are offset to show the different error bars for each data point). Note that orders before No. 10 are measured differently, as discussed in the text, and thus have larger error bars. The diagonal line represents the theoretical expectations for separation of peaks vs. order number, using Equation (6): $\Delta\theta(m) = 0.390\, m$.

3. Conclusions

We have examined the diffraction patterns from two flare events. One of the flares saturated the ADC electronics in the instrument, so we developed a method to extrapolate the intensity of the zeroth order of the flare kernel from the diffraction pattern. The uncertainty of the mean of the extrapolated intensity value was found to be 4.2%. We have checked this method on a second flare that did not saturate the CCD and have confirmed the accuracy of the method to be well within the range of predicted values. This method effectively increases the intensity range of the camera by at least a factor of 41; the zeroth order intensity from even brighter flares than we have analyzed in this paper should be determinable with this method. The light diffracted from the mesh at the front of the telescope was determined to be $\approx$ 20% from the first 23 orders. The ratio of the mesh square slit size to the

slit spacing was accurately determined to be 0.885. We have also demonstrated the visibility of the dispersion effect at sufficiently bright, higher orders, where the separation of two closely spaced wavelengths gradually appears.

Acknowledgements

We thank the referee for helpful comments that improved the paper. We appreciate the encouragement and support from Jake Wolfson. We are grateful to Tom Metcalf for making his diffraction pattern deconvolution procedure available. A. Lin thanks the Lockheed Martin Advanced Technology Center and the Palo Alto Unified School District for allowing him to participate in the Work Experience Program. Work on TRACE data was supported by NASA contract NAS5-38099.

References

Handy, B. N. *et al.*: 1999, *Solar Phys.* **187**, 229.
Hecht, E. and Zajac, A.: 1974, *Optics*, Addison-Wesley Publ. Co., Reading, MA, p. 344.
Schrijver, C. J. *et al.*: 1999, *Solar Phys.* **187**, 261.
Verner, D. A., Verner, E. M., and Ferland, G. T.: 1996, *Atomic Data Nucl. Data Tables* **64**, 1.